

Variability of Track Decay Rate Measurements


Variation of TDR measurements according to EN 15461 on prestressed monoblock concrete sleepers with continuously welded rails 60E1 or 60E2

February 2025

Impressum



Author

Urs Schönholzer,  <https://orcid.org/0000-0001-4333-169X>

Publisher

Allianz Fahrweg Normalspur, Bern, Switzerland, <https://allianz-fahrweg.ch>

ISBN

978-3-907456-01-9

Licence

The contents of this document are licensed under [CC-BY 4.0](https://creativecommons.org/licenses/by/4.0/), unless indicated otherwise.

Link URL

<https://www.allianz-fahrweg.ch/publications/9783907456019.pdf>

Citation

Urs Schönholzer, «Variability of Track Decay Rate Measurements», Allianz Fahrweg Normalspur, Bern, 2025, ISBN 978-3-907456-01-9

<https://www.allianz-fahrweg.ch/publications/9783907456019.pdf>

Version

1.0.0

Internal Reference

PRJ-100-043-202

Content

1	Abstract.....	4
2	Introduction	4
3	Experimental.....	5
4	Results	8
5	Discussion	16
6	Conclusions.....	17
7	References.....	18
	Appendix: Boxplot numerical data	19

1 Abstract

Measuring the track decay rate (TDR) according to EN 15461 is an established practice for assessing the acoustic properties of railway tracks. This measurement is a prerequisite for track sections that are used to assess the pass-by noise of rail vehicles according to EN ISO 3095. Also, in normal operation of railway lines TDR measurements are regularly performed, often in combination with pass-by measurements to assess the noise aspects of railway renewal or expansion projects or to test the effectiveness of noise mitigation measures on the superstructure. Whereas it is common practice to measure several pass-by events to account for the variability of individual trains, TDR measurements are usually just made once per site. This single measurement is then considered to be representative for that site, or sometimes even across individual sites with the same general type of sleepers and rail profiles. There is not much data available about the variation of various individual TDR measurements. This report uses two datasets of repeated TDR measurements by two different suppliers at a total of eight different locations in the Swiss rail network with very similar conditions in terms of track geometry and superstructure. More than 200 third-octave spectra for the vertical and horizontal TDR are present in the data. The variation of the obtained results on nominally identical superstructures is analyzed and discussed.

2 Introduction

Track Decay Rate (TDR) measurements according to EN 15461 are used to characterize the dynamic properties of a section of rail. For the measurement, the rail is excited by hitting it with an impact hammer and it is analysed how the response at a sensor mounted on the rail changes with increasing distance between the impact and the sensor. A track section with high TDR can dissipate the energy of the impact on a rather short distance of rail through the rail fastening system into the sleeper and the rest of the track structure. A rail with a low TDR is not able to dissipate the energy easily and radiates more energy in the form of airborne noise (Thompson, 2009). The rail pads, mounted between the rails and the concrete sleepers, have a significant influence on the TDR. A softer rail pad with a lower static stiffness isolates the rail from the sleeper to a higher extent and results in a lower TDR than a stiff rail pad (Thompson, 2009).

The TDR is mainly a property of the superstructure design that does not change too much over the lifespan of a track. As it is predominantly influenced by the rail pad and the rest of the fastening system it is stable over time if the relevant components do not change their properties over time, for example due to ageing. (Venghaus, 2018). This contrasts with acoustic rail roughness, another parameter defined with a limit curve in EN ISO 3095, that is considered to change more substantially due to developing corrugation over the lifespan of a rail between two grinding cycles (Grassie, 2009). There are several factors that influence the TDR measurement in practice. To perform the measurement, it is possible to keep the location of the impact constant and move the accelerometer sensor farther away with each step (SN EN 15461, 2011). A second possibility is to keep the sensor fixed and to change the position of the impact. The second fundamental choice is the method of fixation of the sensor to the rail. One option is to use glue for this purpose. This takes some time for the glue to cure and to remove the sensor after the measurement is completed. A very easy method of attaching the sensor to the rail is by using a magnetic base plate. But there are some reasonable doubts concerning this method, without prior verification that the sensor attached by the magnet and base plate will show equally well coupling to the rail compared to the fixation by gluing. When the

sensor is fixed by glueing it to the rail, the method with moving the impact position needs to be chosen, as glueing the sensor several times for one measurement is not practically feasible, Another influence on the TDR measurement can be the rail temperature. As nowadays virtually all tracks use continuously welded rail (CWR), the tension within the rail varies with temperature. The target temperature for a non-tensioned rail in Switzerland is 25°C. Below this temperature, tensile forces occur in the rail, above this temperature, compression forces are present in the CWR. Therefore, usually the temperature of the rail, which might differ considerably from the ambient temperature, is recorded during TDR measurements.

TDR is also an input parameter in various models for railway noise prediction (Venkataraman, Rumpler, Leth, Toward, & Bustad, 2022). An intrinsic issue with TDR measurements according to EN 15461 is that the measurement is performed without a train on the track. But the rolling stock influences the coupling of the rail to the sleepers with its weight. The measurement of an unloaded track can underestimate the TDR of the rail underneath a rolling train.

Generally, TDR measurements are expensive, as they need an intervention in track and require the traffic to be closed for operation for the duration of the data acquisition. The actual measurement in track with the sensor and the impact hammer might be done in about one hour. But with installation of the data acquisition electronics and the required cabling, a measurement usually takes half a day on site, in total roughly a day including travel time. Compared with noise measurements this is rather expensive for one set of data. Therefore, it is understandable that repeatability and variability data for TDR measurements is not abundantly available.

The aim of this study is to take the already available measurement data collected over a period of 12 years on the Swiss rail network and to analyze its variability. When reporting the superstructure on which the measurement has been performed, often there is only the sleeper type, and the rail profile specified. It is already clear from theory, that the rail pads also have a major influence. In the data analyzed in the present study, rail pads have been always the same. But there might be other factors that need to be considered or reported.

All data used in the present study comes from measurements on tracks with prestressed monoblock concrete sleepers as described in EN 13230-2 (SN EN 13230-2, 2016) and CWR with vingole rails of a linear weight of 60 kg/m, as-rolled profiles 60E1 and 60E2 according to SN EN 13674-1 (SN EN 13674-1, 2017).

3 Experimental

The present study is based on measurement data that was acquired on the network of Swiss Federal Railways in the years 2012 to 2023. The data was collected at eight locations on the main east-west and north-south railway corridors in Switzerland. In six of these locations, permanent railway noise monitoring stations are operated by the Swiss Federal Office of Transportation. Primary purpose of these sites is the constant surveillance of noise emissions. For quality control, TDR and acoustic rail roughness are measured once per year at all sites.



Figure 1: Photo of a noise monitoring station on the line between the cities of Zürich and Winterthur in Switzerland. The microphones can be seen on the left and right edges of the image. Data acquisition is performed in the gray box in the background, partially covered by the catenary mast on the right side of the track. Photo credit: own work by the author.

3.1 Track Characteristics

All locations included in the study have a double-track normal gauge rail line with the following characteristics

- Tangent track without a substantial gradient
- Rails with a linear weight of 60 kg/m and R260 steel grade, either in 60E1 or 60E2 rolling profile
- Prestressed concrete monoblock sleepers of two subvariants, one for the installation period 1970-1990, another 1991-present. Both variants do not have any under sleeper pads installed. Sleeper spacing is 0.60 m.
- Rail pads made of ethylene-vinyl acetate (EVA) with a static stiffness of about 700 N/mm, colloquially known as “stiff” rail pads. Rail pad thickness is 7 mm.
- Epsilon-type rail clamps of two subvariants (not coinciding with sleeper subvariants).

3.2 Dataset for Supplier 1

The measurements have been performed once a year at the six locations of the noise monitoring stations by one single third-party supplier from 2016 to 2023. Compliance of the measurements with EN 15461 was declared. The method with impact at a fixed location on the rail and moveable sensors was used. Two sensors are moved along the rail to simultaneously measure the signal in both directions from the impact. A third sensor is placed next to the impact hammer to verify the uniformity of the impulse strength introduced into the rail.

Rail temperature was recorded but not included as a factor in the present study. As all measurements were undertaken in the same season, it is concluded that rail temperatures are only varied

mildly. Measurements were taken once each calendar year in the fall, between mid-September and mid-November.

The resulting third-octave spectra are classified by date and by individual rail at all the six measuring sites. The distinction about the two different sleeper types and the two fastening systems were added to be able use them as additional identifiers for each sample in the dataset. For some of the tracks that have been renewed after 2016 the information about the previously installed sleepers could not be determined without doubt. These measurements have been excluded from the results presented in this report.

The dataset consists of 184 third-octave spectra of vertical and horizontal TDR, respectively. For five of the six stations, there is data available for all the eight years from 2016 to 2023 and for all four individual rails. One of the locations has only data for six of the eight years, as there were no measurements taken during an elongated period of track renewal.

3.3 Dataset for Supplier 2

The third-octave spectra have been recorded at a total of six locations and include about 40 third-octave spectra of vertical and horizontal TDR, respectively. Four of these locations with a total of 20 spectra in each direction coincide with four of the locations also measured by Supplier 1. This data was acquired in June and July of 2012. One of the remaining two locations has four spectra and was also measured in the summer of 2012. The bulk of the data for Supplier 2 was measured at one single site with 15 measurements. That site was used for a field study on rail dampers and TDR was measured several times in several sections of about 1 km of tangent track in the years from 2012 to 2015. Only measurements without rail dampers installed were considered for the present study. Supplier 2 uses a manual hammer for the excitation of the rail and leaves the sensor installed in the identical location during the measurement. The hammer is equipped with a sensor to measure the impact force when exciting the rail. The signals of the hammer and at the stationary sensor are monitored during data acquisition and irregular signals are discarded and the measurement at the respective position can be repeated. Compliance with SN EN 15461 has been confirmed.

3.4 General

Data preparation and analysis was performed with the software packages R (R Core Team, 2024) and ggplot2 (Wickham, 2016).

As described above, the rails and rail pads are identical for all measurements. The limit curves of vertical and horizontal TDR according to SN EN ISO 3095 are shown in the plots to guide the eye. The measurements are performed on rails in normal operation, therefore the limit curve for track used for the homologation of vehicles does not apply.

3.5 Simplifications, unconsidered factors

The tracks were in regular use for the entire duration of the study. There were some maintenance activities, such as rail reprofiling or ballast tamping. These events were not recorded and their influence on the TDR spectra was not investigated.

The rails at the measurement sites were installed as a mix of rolling profiles 60E1 and 60E2, based on the time of installation. The difference between the two profiles is minimal. Moreover, the rail-heads are subject to wear from traffic and in addition, material is regularly removed by rail grinding. Therefore, there will not be an exact uniform cross section area of the rails, even if only one single

rolling profile would be present. For the ease of reading, the rail profile is referred to as 60E2 for the remainder of this document.

4 Results

4.1 Dataset for Supplier 1

Figures 2 and 3 show the entire dataset of TDR measurements with a color code applied to differentiate between the two sleeper variants that are present in the data. The red curves are from the newer and current sleeper type that was introduced in 1991. The blueish curves come from the older sleeper variant installed up to that time. It is important to note that this age can only be attributed to the sleeper itself. Rails and rail pads will very likely have been changed once or even multiple times since the older sleepers have been placed in track. It can therefore not be directly concluded that ageing or degradation of the rail pads is a probable root cause for the effects seen below.

The vertical TDR in Figure 2 shows virtually no similarities between all the recorded curves, if the color of the two subsets is ignored and the dataset is viewed in its entirety (see also Figure 7 that only shows the red curves). For the whole frequency range, there are responses in the range of 1 to 30 dB/m present. It looks like any TDR response is possible from the rails under test. The dataset has so much variability, that averaging over all the spectra would give arbitrary results. If the distinction into both subsets is made, the vertical TDR shows no apparent difference of the curves up to the 630 Hz frequency band (upper end of the central horizontal plateau of the black ISO 3095 limit curve). In that lower part, all the curves show substantial variation. In the range between 630 and 2000 Hz, a distinct separation of the two sets is visible, with the older (blue) variant of the sleepers showing a consistently lower TDR. This separation disappears again above 2000 Hz.

Figure 3 shows the horizontal TDR data. There is a much more concise pattern for the measurements, already without the split into the two subsets. A common general trend in the frequency response is visible for the entire dataset. Only at the edges of the relevant frequency range, below 300 Hz and above 3000 Hz, the curves start to diverge. But this is to a smaller extent than for the vertical TDR measurement. Looking at the differences of the two subsets shows a separation only up to the 400 Hz band, with the older sleeper type showing lower decay rates. For the higher frequency bands, there are differences visible, for example in the 3000 Hz band. Just from the general visual impression of Figure 3 it seems that averaging the two individual subset and discussing these two curves could give a meaningful result if the subsets would be compared to each other.

As stated above, it is not the purpose of the analysis to assess compliance of the tracks with the limit curve in EN ISO 3095. It is still noted, however, that except for a few potential outliers at individual frequencies, all the red curves for the horizontal TDR in Figure 3 stay well above of the black limit curve.

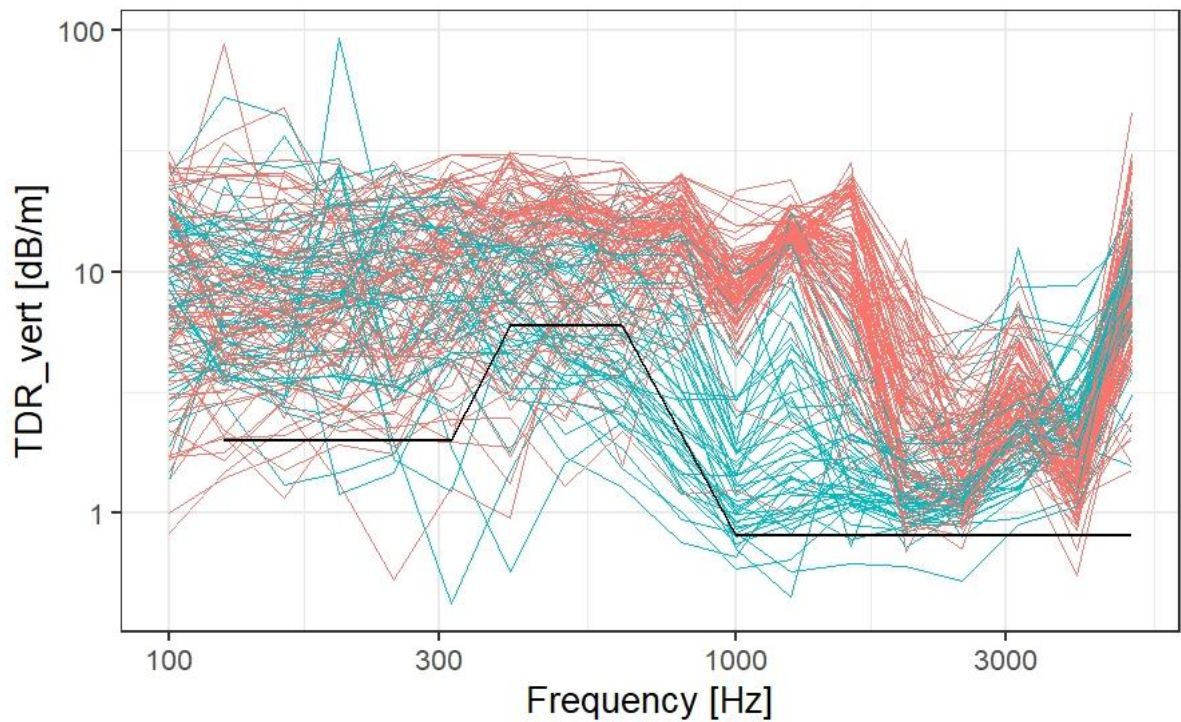


Figure 2: Vertical TDR distinguished by the two types of concrete sleepers in the sample, the red curves are from the newer sleepers younger than 1991, the blue lines are from the older sleepers, $N_{red} = 94$, $N_{blue} = 50$.

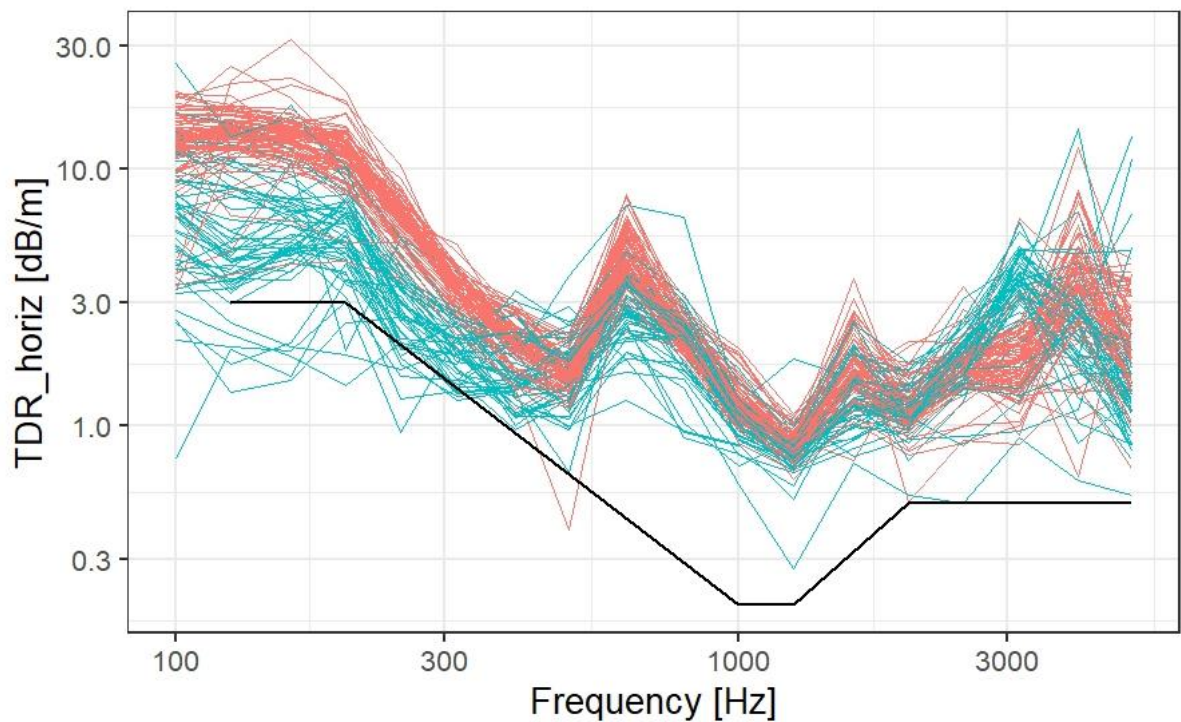


Figure 3: Horizontal TDR distinguished by the two types of concrete sleepers in the sample, $N_{red} = 94$, $N_{blue} = 50$.

Figures 4 and 5 show the red subset from Figures 2 and 3 in the form of boxplots. In this view, the coherence of the single third-octave spectra is lost, and the variation of the collected data is analyzed separately for each of the 18 frequency bands.

The boxplots of the vertical TDR data in Figure 4 show the large spread of the individual values that was already visually apparent in Figure 2. At 800 Hz and below, the boxes are tall and show considerable overlap in horizontal direction. It is probable that a suitable statistical test would lead to the result that there is no significant difference between the individual frequency bands. Just the 1250 Hz band shows a relatively small distribution of values. Above that frequency, the boxes grow very tall again.

Figure 5 with the horizontal TDR data shows quite a strong contrast in the size of the individual boxes compared to vertical data. There is no substantial difference in the spread of the measurement data for all the individual frequency bands present. It is surprising to see such a variation in the distribution of results, given that both the vertical and the horizontal TDR data for each rail have been collected by the same people, at the same dates, with the same equipment.

Numerical values for the bounds of the boxplots can be found in the appendix.

The possibility of TDR variation with time is assessed in Figure 6. The four individual graphs show all four rails of the two tracks at one of the measurement locations. Identical colors of the spectra denote one year of measurement. There is no trend visible for four rails at the location to show an identical variation over time in the lower frequency bands that might offer a time-based explanation for the large spread of measurement values. If degradation of track components was the root cause of the variation, a similar sequence of colors should be visible in the graphs, which is not the case. In addition, the span of eight years is considered a relatively small amount of time, as the life of the components regularly is three times this duration.

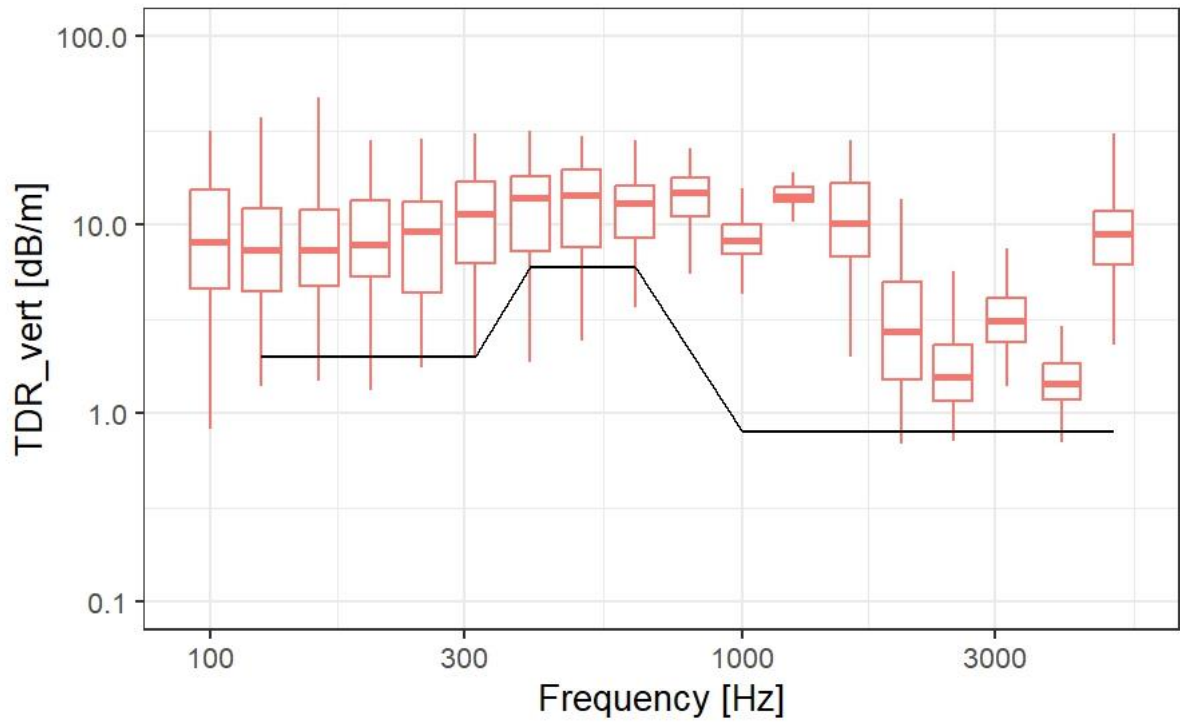


Figure 4: Vertical TDR data of the newer and current version of concrete sleeper (red subset in Figure 2) displayed as boxplots. Outlier points are omitted in the graph for clarity. N = 94.

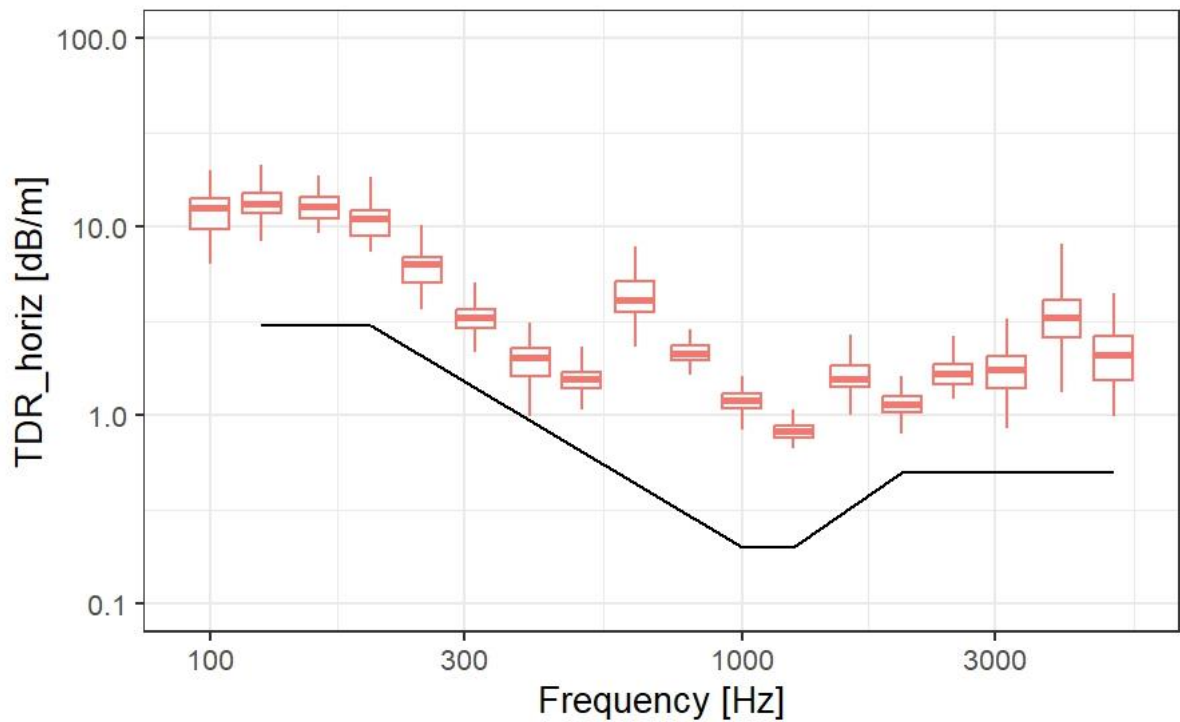


Figure 5: Horizontal TDR data corresponding to Figure 4, scale of the vertical axis identical to Figure 4, N = 94.

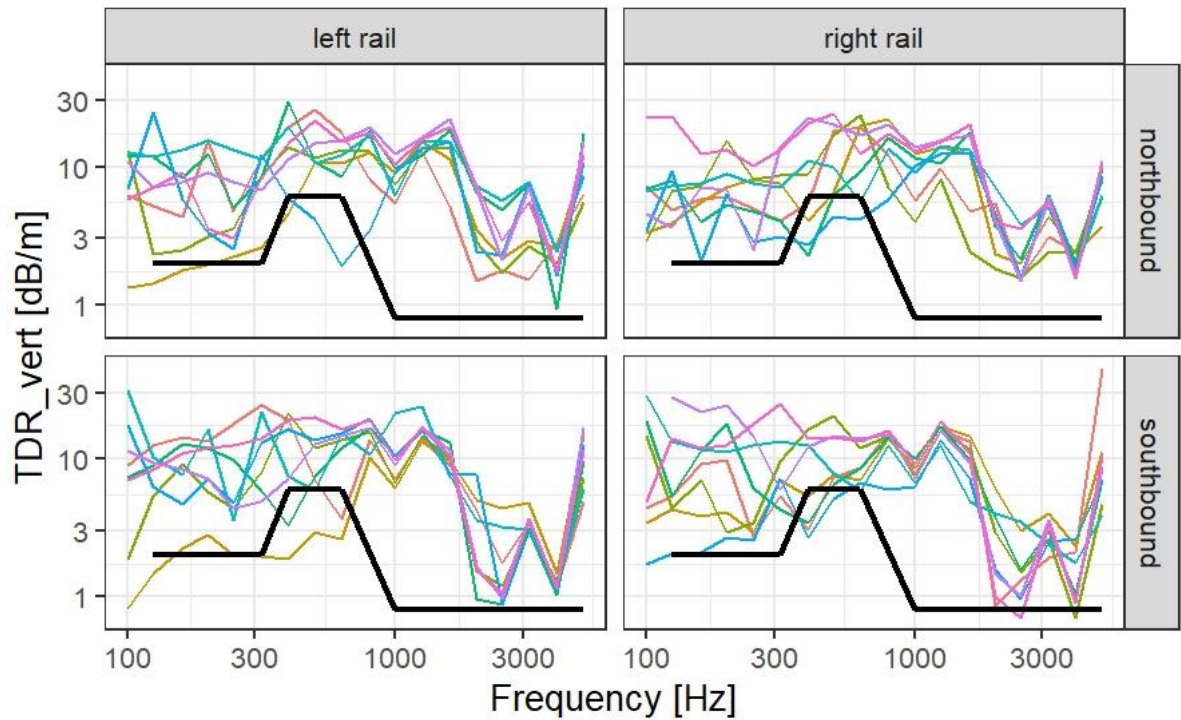


Figure 6: All four individual rails of one station, vertical TDR. Similar color indicates identical year of measurement. N = 8

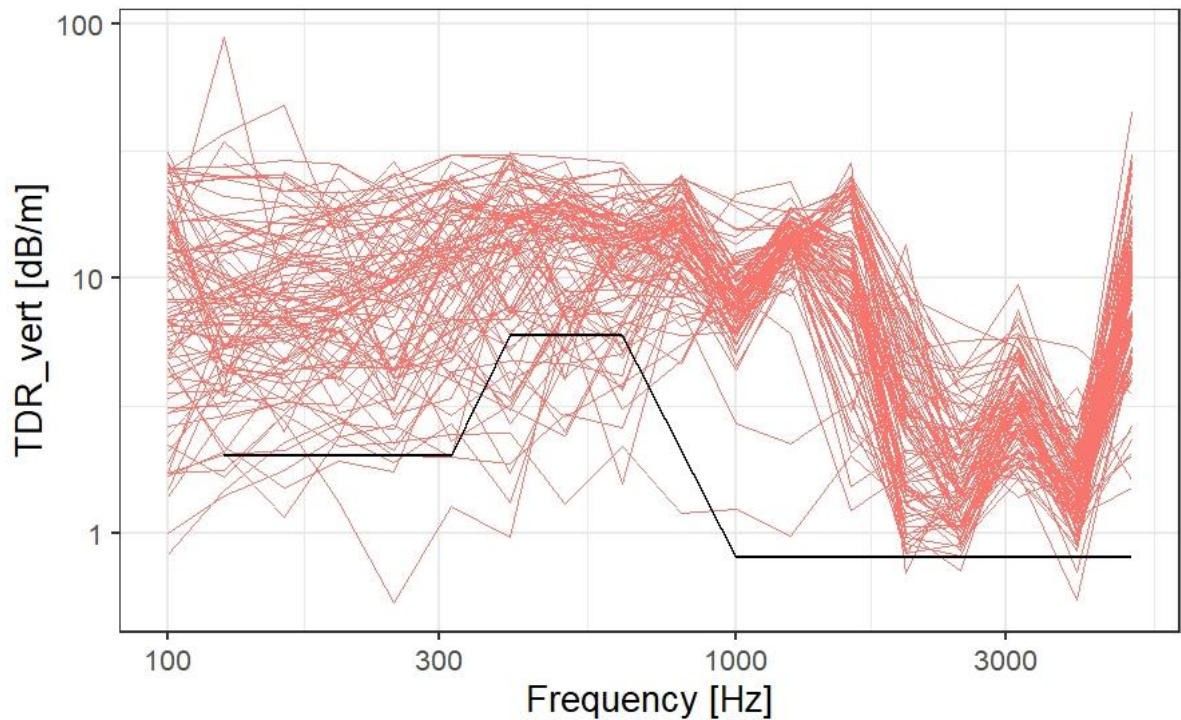


Figure 7: Dataset from Figure 2 with blue lines omitted for visual clarity. N = 94

4.2 Dataset for Supplier 2

The entirety of the second dataset contains third-octave spectra for a variety of sleeper types and suppliers. For this analysis, the focus was placed on a comparison of the variability of measurements on a superstructure identical to the data in the red curves from Figures 4 to 7 measured by a second supplier.

It can be seen in Figure 8 that the variation of vertical TDR in the range from 300 to 1000 Hz is substantially narrower. Even though there are less spectra present in the data the difference seems evident. At frequencies below 300 Hz the variation of the individual spectra becomes larger also in this dataset. The variations for Supplier 2 seem to be a bit larger for frequencies above 1250 Hz.

The variation in the recorded spectra from Supplier 2 for the horizontal TDR in Figure 9 is also smaller than for the measurements in vertical direction. But the difference is considerably smaller than that for Supplier 1.

The Boxplots in Figures 9 and 10 confirm the narrower distribution of the recorded spectra. The numerical values of the boxplot bounds can be found in the appendix.

The data for Supplier 2 also confirms the statement made above that the superstructure under test in the experiments hardly ever crosses the limit curve of SN EN ISO 3095.

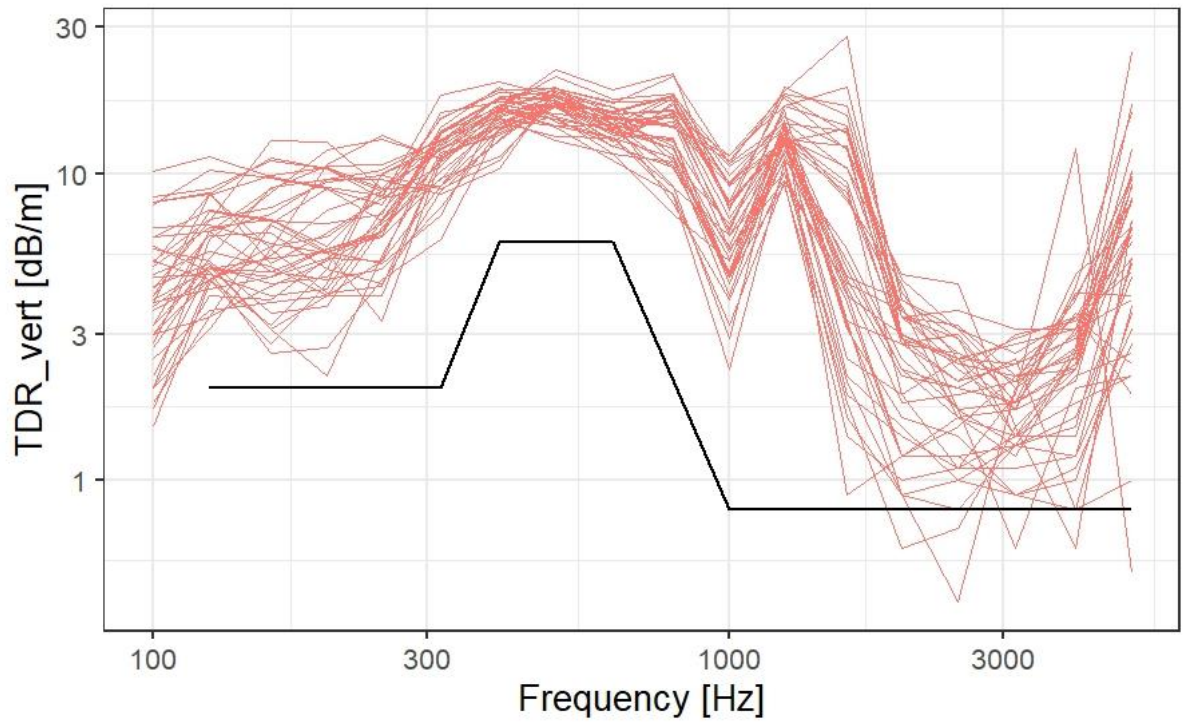


Figure 8: Vertical TDR data measured by Supplier 2. N=40

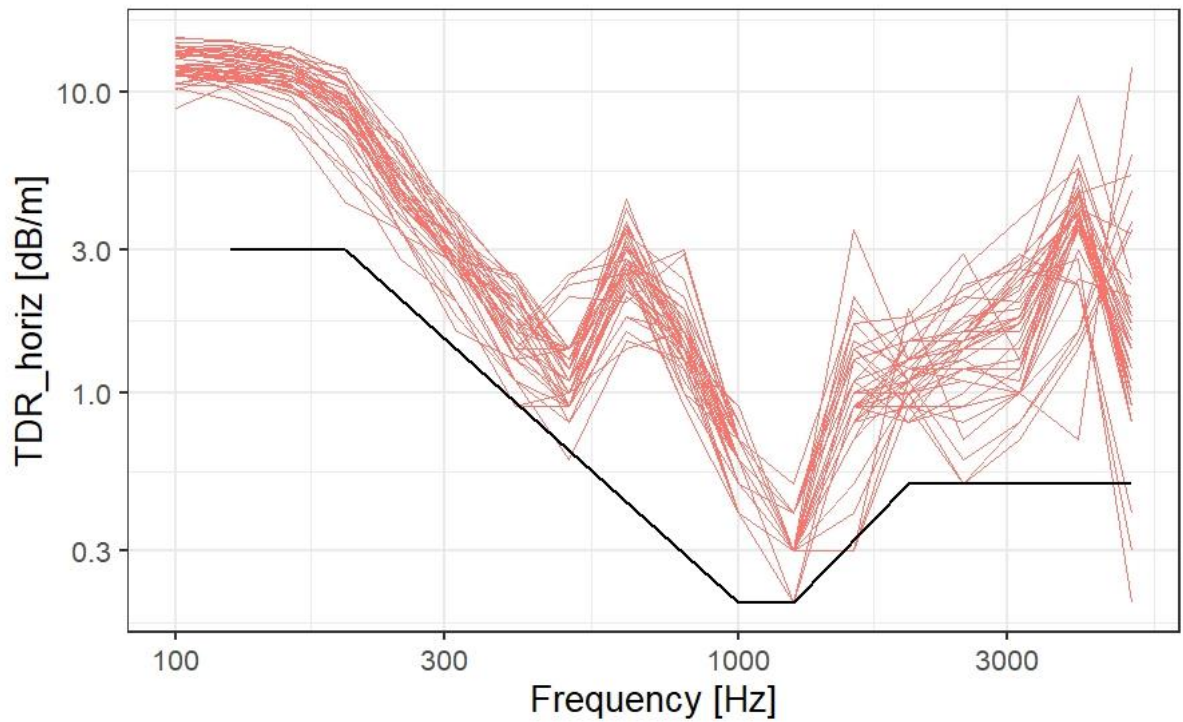


Figure 9: Horizontal TDR spectra for Supplier 2. N = 39

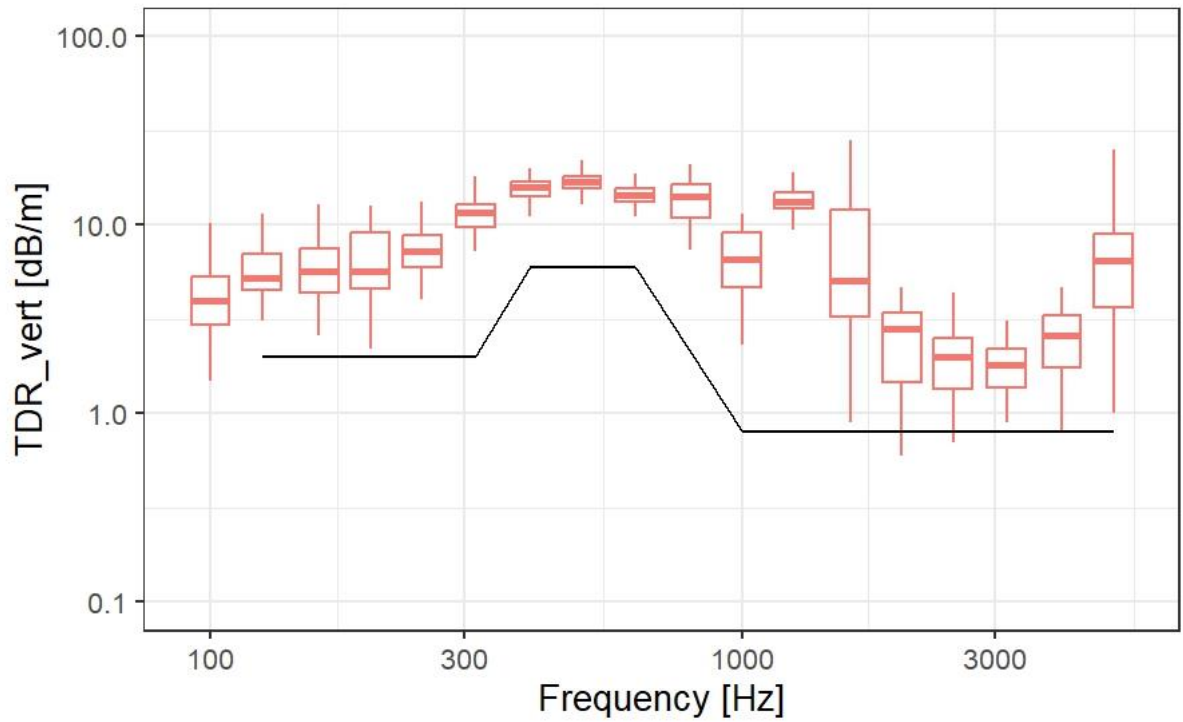


Figure 10: Boxplot of the data shown in Figure 8. Numerical values see appendix. N= 40

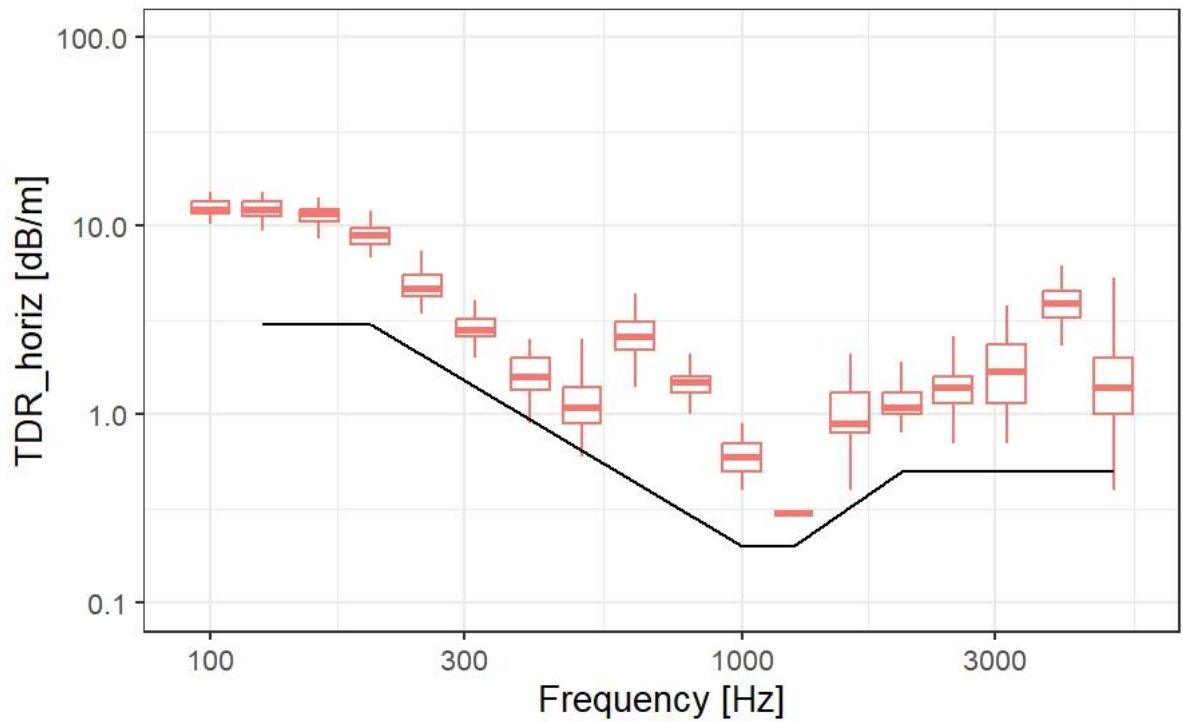


Figure 11: Boxplot of the data shown in Figure 9. Numerical values see appendix. N= 39

5 Discussion

5.1 Variability for sleeper types

Figures 2 and 3 show a significant difference in vertical and horizontal TDR for two types of prestressed monoblock concrete sleepers. The rail profile and rail pads are identical for both types. This systematic difference has been noted in the past, but its root cause has not been comprehensively evaluated. Main reason was that the older sleepers have last been produced around 1990 and track that has been equipped with older production lots from the 1970ies is regularly renewed with the current sleeper type. Therefore, infrastructure managers as well as the authorities did not have a profound interest in finding the root cause of the effect. As the newer sleepers show a higher TDR in both vertical and horizontal direction, this desirable effect was acknowledged, and the origin of the difference was not investigated further.

5.2 Variability of vertical TDR from Supplier 1

The substantial variation of vertical TDR compared to the horizontal values as shown in Figures 2 to 5 has not been found in recent discussions in the field. Of course, one possibility to mitigate the fluctuating vertical values would be calculating the energetic average of the vertical TDR for two rails of a track, or even for the entire dataset. This would visibly eliminate some variation and might be considered the true, or at least more reliable value of the vertical TDR. However, if there is a large statistical component in the results, the resulting average or mean value would not have a significant meaning.

As the boxplot for the 1000 Hz and 1250 Hz bands in Figure 4 are about the same size as all the boxplots for the horizontal TDR, it seems to be possible to achieve a similarly narrow distribution of the measured values, just not for the entire frequency range. Both, vertical and horizontal TDR were measured with the same sensors and the same automated impact hammer has been used. This also means, that the excitation introduced into the rail has been the same for both directions of TDR measurement.

The standard EN 13674-1 defines the dimensions and tolerances for vignole rails. Some other characteristics of the various geometrical cross sections are also listed, for instance the moment of inertia. For the 60E2 rail profile the moment of inertia for a load in vertical direction is given as 3021.5 cm⁴ and for a horizontal load as 510.5 cm⁴. There is a factor of six of difference in the resistance of the rail for bending in vertical or horizontal direction, respectively. If this also effects the transmission of the impulse used for determining the TDR, this means that in vertical direction there is more resistance, and an identical impulse will generate less amplitude in the signal along the rail than in horizontal direction. This would lead to a significantly lower signal to noise ratio for the vertical TDR and could be an explanation for the observed effect. If there is a vertical resonance in the rail in the 1000 – 1250 Hz range, the signal would be strong in that range also for the vertical TDR. This would lead to a much better signal to noise ratio, what could be the reason for the rather narrow spread of values in that range. As the reported dB/m are relative units, there is no conclusion possible about the actual amplitudes that have been recorded by the sensor in the two directions.

The raw data for the measurements was not available for the present study. Therefore, testing this hypothesis could not be done and will be undertaken in further work.

Data collected by Supplier 2 in Figures 7 through 10 show that at least for the range of 300 to 1000 Hz a significantly better overlap of measurements of vertical TDR at various locations with the same superstructure can be achieved. Horizontal TDR seems to be a lot easier to measure for both suppliers.

In the range above 1250 Hz there seems to be the possibility for a systematic difference in average values between measuring methods. The cause for this cannot be assessed with the available data. It would be beneficial to run a round-robin measurement campaign with different contractors to see if the effect of large variation in vertical TDR persists over different teams conducting the measurement according to EN 15461. This has already been done for measurements of acoustic rail roughness according to EN 15610, where results for repeatability and reproducibility are published in TR 15874.

5.3 Use of TDR in Models

It has always been clear that just using the rail profile and concrete sleepers to characterize a superstructure for assessing its TDR is not sufficient. The properties of the rail pads play an important role and the rail pads have to be mentioned as well when reporting on measurements. The present study shows, that also identical rails and rail pads can have a different vertical and horizontal TDR response on two types of prestressed concrete monoblock sleepers. This plays a role when employing models that use a TDR curve as input to determine network-wide noise emissions of railways as for instance mandated by the EU noise directive. If a model uses TDR, all relevant superstructure inventory data needs to be present to calculate the correct emissions and emissions for a railway line. Of course, the error made by for instance using one TDR curve for all concrete sleepers must be put in relation with all other uncertainties of the modelling chain. It does not make sense to meticulously record each type of sleeper in a network when other uncertainties in the modelling chain play a much bigger role.

6 Conclusions

Third-octave spectra measured on comparable superstructure by two different suppliers have found to show a considerable difference in variability amongst individual measurements on tracks with similar components. For a client contracting TDR measurements, it is not possible to assess the quality of different suppliers before or after the measurements. It is unusual to have such a large number of different measurements as a base for an analysis as it was performed here. Before aggregating all the individual measurements over the years, it has not been obvious that the spectra show such a variation. None of the present data has been collected for acceptance tests of rolling stock, but a variation of this magnitude in the data could have an influence if it is also seen with other suppliers. It should mainly be the duty of these suppliers to compare their measurement data over time and use it for quality assurance and plausibility before submitting results to their clients. The root cause for the observed behavior could not be found by analyzing the third-octave spectra. This will require further work and further findings maybe even need to be considered in an upcoming revision of the corresponding standard.

7 References

- Grassie, S. L. (2009). Rail corrugation: Characteristics, causes, and treatments. *Proceedings of the Institution of Mechanical Engineers, Part F: Journal of Rail and Rapid Transit*, 223(6), 581-596. doi:10.1243/09544097JRRT264
- R Core Team. (2024). R: A Language and Environment for Statistical Computing. Vienna, Austria: R Foundation for Statistical Computing. Von <https://www.R-project.org/> abgerufen
- SN EN 13230-2. (2016). *Railway applications - Track - Concrete sleepers and bearers - Part 2: Prestressed monoblock sleepers*. Brussels, Belgium: CEN.
- SN EN 13674-1. (2017). *Railway applications - Track - Rail - Part 1: Vignole railway rails 46 kg/m and above*. Brussels, Belgium: CEN.
- SN EN 15461. (2011). *Railway applications - Noise emission - Characterisation of the dynamic properties of track sections for pass by noise measurements*. Brussels, Belgium: CEN.
- SN EN ISO 3095. (2013). *Acoustics - Railway applications - Measurement of noise emitted by railbound vehicles*. Brussels, Belgium: CEN.
- Thompson, D. J. (2009). *Railway noise and vibration: mechanisms, modelling and means of control*. Amsterdam Boston: Elsevier.
- Venghaus, H. (2018). Ageing Cuts Down the Track Homogeneity Causing Differences Between Calculations and Measurements of Railway Noise. *Noise and Vibration Mitigation for Rail Transportation Systems* (S. 239-249). Cham: Springer International Publishing. doi:10.1007/978-3-319-73411-8_17
- Venkataraman, S., Rumpler, R., Leth, S., Toward, M., & Bustad, T. (2022). Improving strategic noise mapping of railway noise in Europe: Refining CNOSSOS-EU calculations using TWINS. *Science of The Total Environment*, 839, 156216. doi:10.1016/j.scitotenv.2022.156216
- Wickham, H. (2016). *ggplot2: Elegant Graphics for Data Analysis*. New York: Springer-Verlag. Retrieved from <https://ggplot2.tidyverse.org>

Conflict of Interests

The authors declare that they have no competing financial interests or personal relationships that could have influenced the work reported in this document.

Acknowledgements

Swiss Federal Office for Transportation for providing part of the analyzed data.

Appendix: Boxplot numerical data

Outliers are not displayed in the plots but are present here.

Supplier 1 TDR vertical

freq-band	0%	25%	50%	75%	100%
100	0.822	4.61	8.2	15.3	31.5
125	1.39	4.44	7.42	12.3	88.4
160	1.16	4.75	7.39	12	47.6
200	1.32	5.32	7.88	13.6	28
250	0.528	4.39	9.36	13.3	28.6
315	1.27	6.23	11.6	16.9	30.7
400	0.956	7.21	13.9	18.2	31.4
500	1.3	7.58	14.5	19.7	29.8
630	1.56	8.6	13.1	16.3	28.3
800	1.19	11.1	15	17.8	25.5
1000	1.24	6.97	8.21	10	21.6
1250	0.975	13.4	14.2	15.9	24.1
1600	1.23	6.82	10.2	16.8	28.4
2000	0.693	1.51	2.73	4.96	13.6
2500	0.709	1.18	1.56	2.31	6.62
3150	1.38	2.39	3.1	4.13	9.49
4000	0.546	1.19	1.45	1.86	5.38
5000	1.5	6.17	8.96	11.9	45.2

Supplier 1 TDR horizontal

freq-band	0%	25%	50%	75%	100%
100	2.51	9.69	12.7	14.2	20
125	1.35	11.9	13.4	15.1	25.1
160	1.5	11.2	12.8	14.4	31.6
200	1.44	8.98	11.1	12.3	19.9
250	1.66	5.04	6.32	6.96	10.3
315	1.88	2.89	3.34	3.66	5.06
400	0.997	1.62	2.03	2.29	3.09
500	0.394	1.39	1.57	1.71	2.3
630	1.25	3.55	4.1	5.2	7.89
800	0.901	1.98	2.12	2.35	3.16
1000	0.701	1.09	1.21	1.32	2
1250	0.516	0.768	0.829	0.887	1.11
1600	0.73	1.43	1.57	1.85	3.72
2000	0.507	1.04	1.14	1.27	2.11
2500	0.836	1.47	1.67	1.87	3.45
3150	0.849	1.4	1.76	2.07	6.42
4000	0.637	2.57	3.34	4.13	12
5000	0.685	1.55	2.1	2.62	4.45

Supplier 2 TDR vertical

freq-band	0%	25%	50%	75%	100%
100	1.5	2.95	3.95	5.32	10.2
125	3.1	4.5	5.25	7.02	11.4
160	2.6	4.38	5.7	7.5	12.8
200	2.2	4.57	5.65	9.1	12.7
250	3.3	6	7.25	8.83	13.3
315	6.1	9.67	11.6	12.8	18.1
400	10.4	14.2	16	17	19.9
500	12.8	15.6	17	18	21.9
630	11	13.3	14.4	15.6	18.8
800	7.4	10.9	14.2	16.3	21.1
1000	2.3	4.68	6.55	9.12	11.5
1250	9.2	12.3	13.2	14.8	19.1
1600	0.9	3.27	5.05	12	28
2000	0.6	1.48	2.8	3.4	4.7
2500	0.4	1.35	2	2.52	4.4
3150	0.6	1.37	1.8	2.2	3.1
4000	0.6	1.75	2.6	3.32	12.1
5000	0.5	3.65	6.45	9.02	24.9

Supplier 2 TDR horizontal

freq-band	0%	25%	50%	75%	100%
100	8.9	11.6	12.3	13.5	15.2
125	9.4	11.2	12.2	13.4	15
160	7.7	10.6	11.7	12.3	14.2
200	4.3	8	9	9.75	12
250	2.8	4.2	4.7	5.5	7.4
315	1.6	2.6	2.8	3.2	4
400	0.9	1.35	1.6	2	2.5
500	0.6	0.9	1.1	1.4	2.5
630	1.4	2.2	2.6	3.1	4.4
800	0.9	1.3	1.5	1.6	3
1000	0.4	0.5	0.6	0.7	0.9
1250	0.2	0.3	0.3	0.3	0.5
1600	0.3	0.8	0.9	1.3	3.5
2000	0.8	1	1.1	1.3	1.9
2500	0.5	1.15	1.4	1.6	2.9
3150	0.7	1.15	1.7	2.35	3.8
4000	0.7	3.25	3.9	4.55	9.7
5000	0.2	1	1.4	2	12.1